Russian Geology and Geophysics © 2019, V.S. Sobolev IGM, Siberian Branch of the RAS
Vol. 60, No. 9, pp. 1043–1059, 2019 *DOI:10.15372/RGG2019073* *Geologiya i Geofizika*

The Olimpiadinskoe Gold Deposit (Yenisei Ridge): Temperature, Pressure, Composition of Ore-Forming Fluids, $\delta^{34}S$ in Sulfides, $^{3}He/^{4}He$ of Fluids, Ar–Ar Age, and Duration of Formation[1]

N.A. Gibsher[a, ✉], A.A. Tomilenko[a], A.V. Sazonov[b], T.A. Bul'bak[a], M.A. Ryabukha[a], S.A. Sil'yanov[b], N.A. Nekrasova[b], M.O. Khomenko[a], E.O. Shaparenko[a]

[a] *V.S. Sobolev Institute of Geology and Mineralogy, Siberian Branch of the Russian Academy of Sciences, pr. Akademika Koptyuga 3, Novosibirsk, 630090, Russia*

[b] *Siberian Federal University, School of Mining, Geology and Geotechnology, pr. Svobodnyi 79, Krasnoyarsk, 660041, Russia*

Received 23 August 2018; received in revised form 25 December 2018; accepted 5 February 2019

Abstract—New thermobarogeochemical and isotope-geochemical data are presented, which show the intricate and long history of the formation of the unique Olimpiadinskoe gold deposit with predicted gold reserves of >1000 tons on the Yenisei Ridge. Metal-bearing oxidized water–carbon dioxide and reduced carbon dioxide–hydrocarbon fluids participated (at the same time or successively) in the formation of the deposit at 220–470 ºC and 0.6–2.5 kbar. Fluids of gold-bearing mineral assemblages include CO_2, hydrocarbons, and S-, N-, and halogen-containing compounds capable of transporting ore elements, including gold. Highly mobile carbon dioxide–hydrocarbon fluids were responsible for the appearance of disseminated gold mineralization in large bodies of quartz–carbonate–mica schists serving as geochemical barriers in the Olimpiadinskoe deposit. The deposit formed in the period from 817 to 660 Ma, which fits the time interval from crystallization to cooling (868–721 Ma) of the most proximal multiphase Chirimba granitoid pluton. The hydrothermal activity of the fluids that formed the Olimpiadinskoe deposit lasted at least 100–150 Myr year.

Keywords: fluid inclusions, quartz, gold, hydrocarbons, Ar–Ar age

INTRODUCTION

Currently, the gold mining industry of Russia is mainly concentrated on the gold ore deposits with disseminated and veined-disseminated ores in carbon-carbonate-terrigenous rocks. These objects with moderate or low gold contents with significant volumes of ores allow high-performance quarrying (Li, 2003; Novozhilov et al., 2014). The specificity of this type of deposits is that a greater part of the gold is represented by dispersed particles and spread out in a large volume of metasomatic rocks. The Olimpiadinskoe deposit is a representative of this type on the Yenisei Ridge, which is comparable in reserves with such gold ore giants as Sukhoi Log, Natalka, Muruntau, Kumtor, Kulgurli, Bendigo, etc. (Li, 2003; Serdyuk et al., 2010; Novozhilov et al., 2014; Groves et al., 2016; Sazonov et al., 2016).

Genetic reasons for the localization of gold mineralization at separate levels of the section of ore-bearing rocks are debatable. In some genetic models, primary enrichment of sediments with clastogenic gold in terrigenous sediments, or chemogenic, is allowed due to submarine hydrothermal activity near the joints of basement faults, which were repeatedly renewed and controlled the placement of hydrothermal mineralization. (Petrov, 1974; Buryak, 1982). Other researchers (Novozhilov and Gavrilov, 1999; Li, 2003; Kryazhev and Grinenko, 2007; Novozhilov et al., 2014; Kryazhev, 2010, 2017; Sazonov et al., 2010) suggest that deposits of Sukhoi Log–Olimpiadinskoe type are hydrothermal, and the fluid systems are associated with magmatogenic or metamorphogenic processes. In this case, the formation of gold-bearing metasomatites, distribution, and concentration of ore substance, including gold supply, was carried out by hydrothermal solutions from deeper sections of the Earth's crust, which finally resulted in thick and extended ore bodies. In hydrothermal models, ore-forming fluids of the Yenisei deposits play the main role in gold ore genesis (Prokof'ev et al., 1994; Afanas'eva et al., 1995; Baranova et al., 1997; Genkin et al., 2002).

In recent years, the improvement of traditional and application of new methods and the latest generation devices made it possible to refine the earlier obtained physicochemical parameters of fluids and use them for practical purposes, geological exploration works at deep horizons of the Olimpiadinskoe deposit, search and evaluation in other gold regions.

[1] This paper was translated by the authors.

✉ Corresponding author.
E-mail adress: gibsher@igm.nsc.ru (N.A. Gibsher)

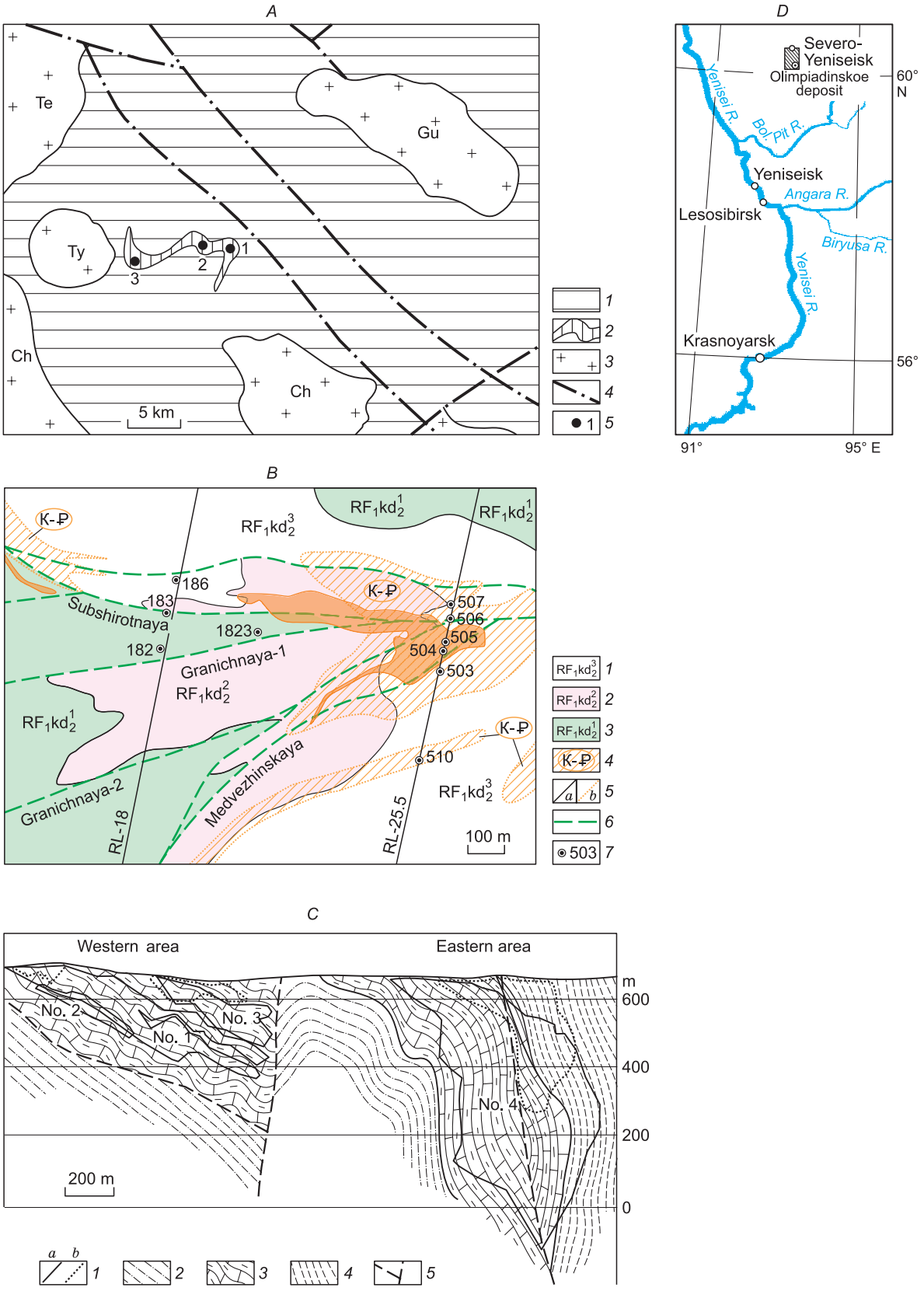

Fig. 1. Geological structure of the southern part of the Northern Yenisei ore region (Sazonov et al., 2016) (*A*); Geological structure of the Eastern part of the Olimpiadinskoe gold-ore (Sazonov et al., 2016) (*B*); Projection of ore bodies of the Olimpiadinskoe deposit on a vertical plane (Li, 2003) (*C*); geographical position of the deposit (*D*). *A*: *1*, crystalline schists of biotite zone (Lower Riphean, Sukhoi Pit Series, Korda Formation);

In this study we used a collection of samples from exploration works in 2009–2014 at the Olimpiadinskoe deposit and fluid inclusion studies at other gold ore occurrences of the Yenisei Ridge (Tomilenko and Gibsher, 2001; Gibsher et al., 2011, 2017; Ryabukha et al., 2015; Tomilenko et al., 2010), with the main focus on the description of gold mineralization factors of fluids which formed the unique Olimpiadinskoe deposit. We have carried out a complex of thermobarogeochemical studies of fluid inclusions in quartz, sulfides and carbonates, obtained data on the characteristic of isotope composition of sulfide sulfur, helium isotopes in fluid inclusions, and determined the composition and concentrations of platinum group elements, Ar–Ar age and duration of the formation of the Olimpiadinskoe deposit.

BRIEF GEOLOGICAL AND MINERALOGICAL CHARACTERISTICS OF THE OLIMPIADINSKOE GOLD DEPOSIT

The Olimpiadinskoe deposit of disseminated gold-sulfide ores is the largest of the gold ore occurrences being explored at the present time in the Yenisei Ridge. This section is written on the basis of published materials of one of the pioneers of the Olimpiadinskoe deposit L.V. Li (Li et al., 1984; Li, 2003), and later works (Sazonov and Kremenetskii, 1994; Sazonov et al., 2016; Genkin et al., 1994, 2002; Serdyuk et al., 2010; Novozhilov et al., 2014). The deposit is located in the southern part of the Northern Yenisei Ridge ore region, on an area of a tectonic block with a subsided roof of a granitoid batholith. On the day surface the granitoids are exposed as the large Chirimba pluton and other small intrusions that surround the deposit in the form of a half ring (Fig. 1*A*). The deposit lies in the area of dynamic effect of the Tatarka deep-seated fault. According to the modern stratigraphic scheme adopted for the region, the ore-bearing formation is attributed to the Korda Formation of Sukhoi Pit Series of the Riphean (Fig. 1*B*). Ore-bearing rocks undergo metasomatic changes (silicification, carbonatization, sericitization and chloritization) that preceded and accompanied the formation of early quartz–gold–arsenopyrite-pyrrhotite (±scheelite) and later quartz–gold–antimony (±scheelite) mineral associations.

The features of geologic development characterized by increased tectono-magmatic activity determined the metallogenic specifics of the Olimpiadinskoe deposit. A peculiar feature of the deposit is the distribution of gold–pyrrhotite–arsenopyrite, gold–wolframite, gold–scheelite, gold–antimonite and gold–bismuth mineralization within its ore field, which differs from the gold–quartz mineralization that is typomorphic for the Yenisei Ridge.

The hydrothermal process in the ore field of the deposit started from the formation of metasomatites of various compositions at the pre-ore stage, continued at the ore stage by the deposition of gold ore mineralization and finished by the crystallization of quartz ± calcite ± fluorite ± feldspar veinlets at the post-ore stage. The main component in all types of hydrothermal mineralization is gold, but there are also increased amounts of tungsten, silver and antimony. The distribution of veinlet-disseminated ore bodies is controlled by a system of discontinuous interstratal faults that complicate the periclinal closing of the Medvezhinskaya anticline. The material composition of ores is quartz, carbonates, mica (muscovite, sericite, biotite). The ores also contain minor chlorite, rutile and dispersed carbonaceous substance (from thousandths fractions to 1–2%, in places reaching 4.15%). The deposit consists of two interconnected areas: Western (Zapadnoe) (or Olimpiadinskoe) and Eastern (Vostochnyi) (Pravoberezhnyi), differing in the specifics of structural position and scale of mineralization (Fig. 1*C*). Three ore bodies (Nos. 1, 2, 3) were identified in the Western area, and one, main, body (No. 4) in the Eastern area, where more than 90% of the gold is concentrated. The ore bodies of the deposit are confined to carbonate-bearing stratified packs and are contoured by sampling. These are metasomatites of predominantly mica–carbonate–quartz and zoisite–feldspar–quartz–mica composition, containing dissemination, veinlets of ore minerals and microscopic particles of gold (Li, 2003; Novozhilov et al., 2014). The inner structure of ore bodies is heterogenous. Gold-rich ore layers, bands and lenses in them alternate with ore-poor and barren parts. Gold-enriched parts are confined to fault zones with intensely developed mineralization of arsenopyrite, pyrrhotite and antimonite–berthierite. The maximum vertical range of mineralization is estimated at more than 1400 m.

Gold is the main useful component of ore at the deposit and occurs mostly as dispersed particles. The main gold concentrator is arsenopyrite of needle-like habit, and short-prismatic and coarser grained pseudospiral varieties of arsenopyrite contain about 1–3 orders of magnitude less gold than the needle-like variety (Li, 2003; Novozhilov et al.,

2, Upper Enashima ore-bearing zone of local dynamothermal metamorphism; *3*, granitoid plutons: Gu, Gurakhta; Ty, Tyrada; Ch, Chirimba; Te, Teya; *4*, faults; *5*, gold deposits: 1, 2, Olimpiadinskoe (1, Vostochnoe, 2, Zapadnoe), 3, Tyrada. *B*: 1–3, Early Riphean deposits of the Sukhoi Pit Series, Middle Korda Subformation: *1*, third member ($RF_1kd_2^3$): carbonaceous, quartz-sericite and carbonate-quartz-mica schists, mica-quartz-carbonate and mica-carbonate-quartz apocarbonaceous metasomatites; *2*, second member ($RF_1kd_2^2$): quartz-carbonate-mica schists with horizons of marmorized limestones, carbonate-quartz-zoisite-mica, mica-carbonate-quartz metasomatites within ore bodies; *3*, first member ($RF_1kd_2^1$): biotite-quartz and quartz-muscovite schists with garnet, horizons of mica quartzites at the base; *4*, crusts of weathering and their age; Korda Formation rocks and Tatarka–Ayakhta complex granitoids with different degrees of weathering; variegated gravelly-sandy, sandy-clayey and clayey formations, including argillizites; *5*, geologic boundaries (*a*, between subdivision of various ages; *b*, crusts of weathering); *6*, systems of interstratal faulting; *7*, numbers of wells. RL-18 and RL-25.5, exploration lines. *C*: *1*, boundary of primary (*a*) and oxidized (*b*) ores; *2*, quartz-mica schists; *3*, quartz-carbonate mica schists with layers of carbonate rocks; *4*, carbonaceous schists; *5*, faults.

2014). Less frequently, gold was found in pyrrhotite, pyrite, Sb-bearing minerals as well as in microgranoblastic quartz and micas of the groundmass of ore-bearing rocks. Pyrrhotite, closely related to gold, occurs as tiny particles in metasomatites after quartz-carbonate-mica schists in the form of nests and veinlets, frequently of large sizes in quartz-gold-sulfide veins.

Gold-antimony, accompanied by tellurides, mineralization consisting of predominant antimonite and berthierite is distributed locally and spatially isolated in the zone of the Medvezhinskoe ore-controlling fault. This mineralization is referred to late productive formation superimposed on the early quart–gold–arsenopyrite–pyrrhotite mineralization. Scheelite mineralization also occurs locally and is associated with skarnoids, carbon-mica-carbonate metasomatites (Afanas'yeva et al., 1995).

Quartz is the main mineral that constantly occurs in pre-ore metasomatites, gold-sulfide mineral association and post-ore quartz–carbonate ± feldspar ± fluorite formations. Several generations of quartz have been distinguished at the deposit.

Quartz-I is developed in pre-ore metasomatites. It makes up thin veinlets, nests and lens-shaped segregations filled with fine-grained white quartz. The grains of quartz show traces of plastic deformations in the form of blocky, linear and wavy extinction. Among newly formed minerals associated with quartz are scales of muscovite, biotite, sericite and impregnated sulfides. Gold content in the studied pre-ore metasomatites is no more than 0.3–0.4 ppm.

At the ore stage, two generations of quartz (quartz II and III) were revealed. Quartz II occurs in gold–arsenopyrite–pyrrhotite mineral association, and quartz III, in gold-antimony association. Quartz of generation III, typically, fills single veins and nests in fracturing and compression zones.

Quartz of generation IV composes systems of thin quartz and quartz–carbonate ± feldspar ± fluorite veins that intersect pre-ore metasomatites and quartz-gold-sulfide ores of the deposit.

FACTUAL MATERIAL AND METHODS OF STUDY

The factual material is based on the collection of 70 samples. The studied samples were taken along prospecting lines 18.0 and 25.5 (Fig. 1*B*) from 10 wells in the range of depths from 4.5 m (well 503) to 817 m (well 510) of ore body No. 4 in the Eastern part of the deposit (Fig. 1*C*). Petrographic sections and plates polished from both sides were made from one of the samples to study individual fluid inclusions, and the second half of the same sample was crushed and sieved. The description of the procedure for preparing the samples for analysis is given in (Gibsher et al., 2011). The temperature of total homogenization, eutectics and melting of ice of water solutions, temperature of partial homogenization and melting of $CO_2 \pm CH_4 \pm N_2$ gases in fluid inclusions were measured in a Linkam THMSG-600 microscope microthermal chamber in the range of temperatures from –196 to +600 °C. Standard measurement error is ±0.1 °C in the negative and ±5 °C in the positive regions of temperature.

The pressure of fluid in the hydrothermal system was estimated from syngenetic inclusions (L_{H_2O} + G, $L_{CO_2 \pm CH_4 \pm N_2}$, $G_{CO_2 \pm CH_4 \pm N_2}$). The gas-liquid inclusions were used to measure the total homogenization temperature, and carbon dioxide-methane-nitrogen inclusions, to determine the temperature of partial homogenization and type of homogenization (in liquid or gas phase). The obtained parameters allow estimation of fluid pressure by the procedures reported in (Brown and Lamb, 1989; Thiéry et al., 1994; Duan et al., 1996; Bakker, 2001). The water phase composition of individual fluid inclusions was determined on the basis of eutectic temperatures that characterize the water–salt system (Borisenko, 1977). The salinity of solutions was estimated from the melting temperature of ice and dissolution temperature of salt crystal, using the two-component water–salt system NaCl–H_2O (Kirgintsev et al., 1972). The composition and concentration of platinum group elements (PGE) and rhenium in fluid inclusions of quartz and sulfides were determined by inductively coupled plasma mass spectrometry (ID-ICP-MS). The procedure for preparing the substance from fluid inclusions in sulfides and quartz is described in (Kozmenko et al., 2011; Gibsher et al., 2018).

The gas phase composition of individual fluid inclusions was analyzed on the single channel Ramanor U-100 Raman spectrometer by Jobin Yvon, using an argon laser with a diameter of 1.5 μm and power 3 W by the procedure reported in (Dubessy et al., 1989). The bulk composition of gas component was determined using gas chromatography-mass spectrometry (GC-MS). The mineral was placed into a special device included into the gas scheme of the chromatograph before the analytical column. The gas phase from fluid inclusions was extracted without pyrolysis at a single shock destruction of the sample in the inert helium flow. The detailed description of the GC-MS method is given in (Tomilenko et al., 2015; Sokol et al., 2017). No organic substances were used at any stages of preparation of samples for analysis.

Sulfur isotopes ($\delta^{34}S$) of sulfides were measured in SO_2 gas obtained by the interaction of sulfides with CuO at 1000 °C and normalized with respect to isotope composition of troilite from the Diablo Canyon meteorite. The reproducibility of $\delta^{34}S$ values, including sample preparation, is 0.1‰ (Pal'yanova et al., 2016).

The isotope composition of helium in fluid inclusions of quartz was determined in the laboratory of Geochronology and Geochemistry of Isotopes in the Geological Institute of the Kola Scientific Centre (Apatity, RAS). Methodical techniques are described in (Tolstikhin and Prasolov, 1971; Vetrin et al., 2003; Ikorsky et al., 2006, 2014).

Isotope-geochronological data (16 samples) were obtained on the Ar–Ar dating of potassium-bearing minerals from muscovite of near-vein metasomatic rocks with minor contents of Au, As and Sb; from muscovite and sericite of

quartz–gold–arsenopyrite–pyrrhotite associations with gold content from 0.6 to 16.2 ppm, As from 0.02 to 1.86% and Sb from 0.0 to 0.01%; from sericite of quartz–gold–antimony associations with gold content from 0.3 to 21.6 ppm, As from 0.02 to 11.5% and Sb from 0.01 to 4.42%. The monomineral fractions of sericite and muscovite were picked manually under a binocular magnifying glass. The purity of fractions was controlled microscopically in mounted sections and on a scanning microscope. The description of analytical procedures is reported in (Travin, 2016).

RESULTS

Characteristics of fluid inclusions. Individual fluid inclusions were studied in quartz of pre-ore metasomatites, early gold-arsenopyrite ± pyrite ± pyrrhotite and later gold-antimony parageneses united into ore stage, as well as in quartz-carbonate veinlets of post-stage.

In quartz from the Olimpiadinskoe deposit four types of fluid inclusions were revealed at room temperature (Fig. 2):

(a) gas-liquid (L_{H_2O} + G) with varying volume ratios of liquid and gas in inclusions in the range from 70:30 to 20:80, respectively (Fig. 2*A*);

(b) water-carbon dioxide (L_{H_2O} + $L_{CO_2 \pm CH_4 \pm N_2}$). In these inclusions the ratio carbon dioxide (gas or liquid CO_2) and water phase varies from 90:10 to 20:80, respectively (Fig. 2*B*);

(c) water-salt type (L_{H_2O} + G + CR) (Fig. 2*C*), which contains a daughter salt crystal of cubic habit.

(d) single-phase liquid or gas methane-carbon dioxide, nitrogen-methane-carbon dioxide, methane and nitrogen inclusions (L_{CO_2}; $L_{CH_4+N_2+CO_2}$; L_{CH4}; G_{CH_4}; G_{N_2}; $G_{CH_4+N_2+CO_2}$) (Fig. 2*D*).

Inside quartz grains of gold-bearing associations one can occasionally observe shapeless black particles surrounded by methane-nitrogen-carbon dioxide gas inclusions (Fig. 2*E*). There also occur black rounded globules, which are, according to Raman spectroscopy data, composed of fine-dispersed carbon (Fig. 2*F*).

Quartz grains (I generation) from nonauriferous pre-ore metasomatites contain conserved small (5–10 μm) fluid inclusions of (L_{H_2O} + G) and (L_{H_2O} + L_{CO_2} + G) types. The fluid inclusions are either regularly scattered in the quartz, or form groups of 5–10 inclusions that are not confined to healed fractures. We refer these inclusions to the primary of pseudosecondary formations. In addition to primary fluid inclusions, quartz I contains two types of secondary inclusions. The first type is gas-liquid inclusions in which the liquid phase (L_{H_2O}) is permanently predominant. These inclusions are confined to a large number of healed fractures that intersect the boundaries of quartz grains. Numerous fractures decorated with submicron (1–5 μm) secondary inclusions are often grouped into curved bands and in places intersect with each other. Quartz at these sites has a wavy block extinction.

The second type of inclusions (Fig. 2*D*) is filled with substantially gas (or dense liquid) carbon dioxide-methane-nitrogen fluids that are confined to healed fractures dissecting the boundaries of quartz grains. This type of inclusions has a more diverse but frequently an elongated shape of vacuoles and their sizes (20–40 μm) significantly exceed the sizes

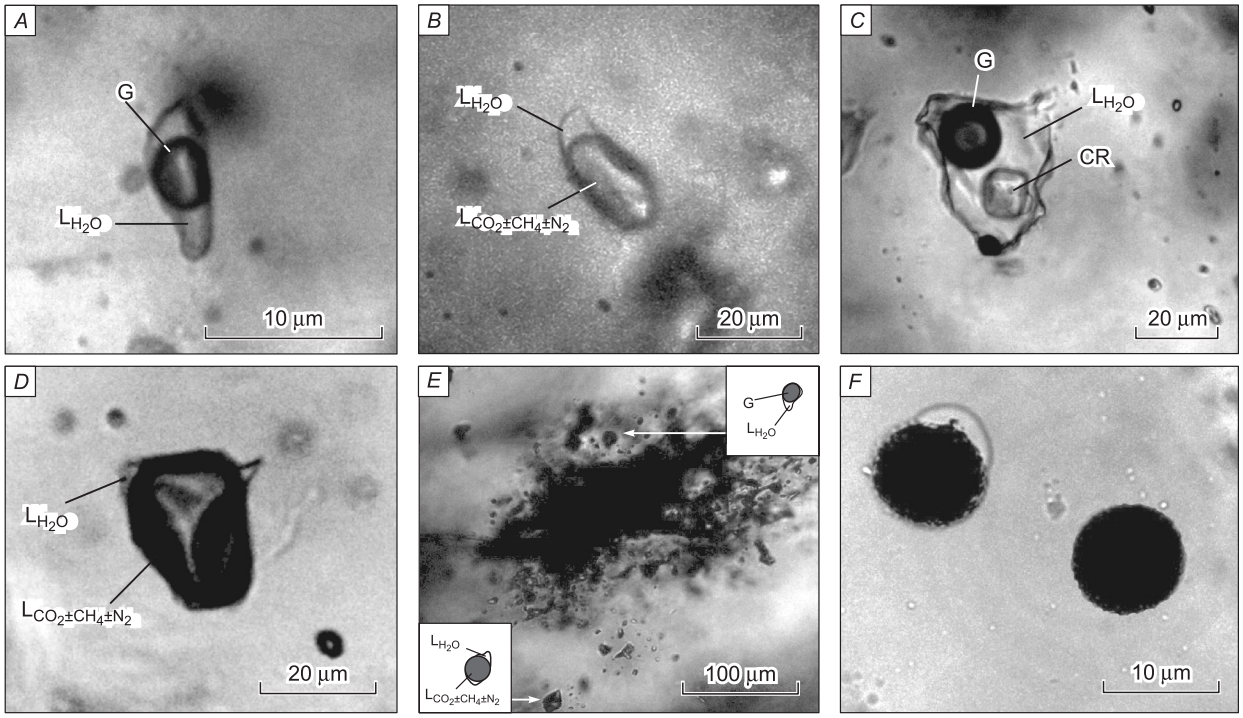

Fig. 2. Types of fluid inclusions in quartz from the Olimpiadinskoe deposit. L, liquid, G, gas, CR, crystal. Explanations are in the text.

of primary and pseudosecondary inclusions. When viewed under the microscope in transmitted light, these inclusions appear dark (black). When the temperature decreases, a thin border of liquid water appears at the boundary of the vacuole and host mineral, which freezes at –40 °C.

Gas-liquid inclusions with varying ratios of phases are conserved in the quartz-gold-sulfide associations of quartz II. In the same group with gas-liquid inclusions in quartz II there are also inclusions with carbon dioxide, methane and nitrogen, which are not confined to healed cracks. We refer these groups of inclusions to syngenetic formations. In quartz of generation II we found numerous intersecting cracks, during healing of which large (20–40 μm) gas inclusions were trapped. Healed cracks with gas inclusions cut the boundaries of quartz grains. Based on this fact, we referred them to secondary formations. Occasionally, second generation quartz contains small (<5–10 μm) inclusions with a salt crystal (Fig. 2*C*), which also tend to healed cracks, intersecting with the cracks filled with gas inclusions. The inclusions with daughter crystals were referred to secondary formations. Quartz II of the ore stage (well 1823, at depths from 523.8 from 601.8 m) contains particles of carbonaceous substance surrounded by gaseous methane-nitrogen-carbon dioxide inclusions (Fig. 2*E*).

In quartz III from gold-antimony mineral association there are mainly gas-liquid (L_{H_2O} + G) inclusions in which the volume of liquid water phase is larger than that of the gas phase. Less frequently, they occur together with carbon dioxide inclusions. Based on their arrangement in quartz grains and lack of confinement to healed cracks, we referred these inclusions to primary formations. Quartz III also contains secondary inclusions filled with a mixture of methane, nitrogen and carbon dioxide in different proportions.

Post-ore quartz (generation IV) and calcite from thin quartz-carbonate veinlets contains only gas-liquid (L_{H_2O}>>G) primary inclusions whose size rarely exceeds 5–10 μm.

Homogenization temperature of fluid inclusions, composition, salinity and pressure of fluids. Results of thermometric and cryometric studies of fluid inclusions in quartz

Table 1. Summarized results of microthermometric studies of fluid inclusions in quartz from the Olimpiadinskoe gold-ore deposit

Generation of inclusions	Total homogenization *T*, °C	Type of homogenization	Crystal dissolution *T*, °C	Eutectic *T*, °C	Melting temperature of ice, °C	Salinity, wt.% NaCl-equiv.	Melting temperature of $CO_2 \pm CH_4 \pm N_2$, °C	Partial homogenization *T* of $CO_2 \pm CH_4 \pm N_2$, °C	Type of homogenization	*P*, kbar
Nonauriferous quartz–mica–sulfide associations										
P, PS	$\frac{220-325}{290}(92)$	L	–	$\frac{-24.5\div-28.0}{-26.3}(40)$	$\frac{-6.3\div-11.0}{-8.0}(35)$	$\frac{10-16}{12.5}$	–57.0÷–59.3	–4.2÷–8.5	G, L	
S-b	–	–	–	–	–	–	–58.4÷–69.1	–8.5÷–140.0	L, G	0.6–2.2
S-d	$\frac{140-190}{150}(23)$	L	–	$\frac{-10.3\div-20.0}{-12.0}(15)$	$\frac{-0.5\div-2.0}{-1.5}(15)$	$\frac{1-4.5}{3}$	–	–	–	
Quartz–gold–arsenopyrite ± pyrite ± pyrrhotite associations										
P, PS	$\frac{260-470}{350}(125)$	L, G, G–L	–	$\frac{-29.4\div-33.8}{-31.5}(30)$	$\frac{-5.4\div-17.0}{-11.0}(25)$	$\frac{9.5-20}{16}$	–56.9÷–71.0	–0.5÷–122.5	G, L	
S-b	–	-	–	–	–	–	–70.3÷–81.0	–20.3÷–113.0	G, L	
S-c	$\frac{160-240}{180}(17)$	L	$\frac{150-230}{175}(15)$	$\frac{-49.0\div-55.6}{-52.3}(10)$	$\frac{8.0-14.5}{-10.3}(10)$	>30	–	–	–	1.1–2.5
S-d	$\frac{150-210}{180}(29)$	L	–	$\frac{-9.3\div-19.0}{-16.3}(15)$	$\frac{-0.3\div-1.5}{-1.0}(13)$	$\frac{0.5-3}{2}$	–	–	–	
Quartz–gold–antimony associations										
P, PS	$\frac{240-300}{260}(89)$	L	–	$\frac{-27.3\div-30.4}{-28.5}(35)$	$\frac{-2.8\div-4.0}{-3.5}(30)$	$\frac{5.5-8}{7}$	–59.3÷–60.3	–7.3÷–14.5	L	
S-b	–	–	–	–	–	–	–58.4÷-69.8	–6.5÷–135.4	G, L	1.8–2.1
S-d	$\frac{120-190}{150}(41)$	L	–	$\frac{-12.5\div-18.9}{-16.0}(21)$	$\frac{-0.3\div-2.5}{-1.7}(15)$	$\frac{0.5-5}{3.5}$	–	–	–	
Quartz–calcite association										
P, PS	$\frac{110-180}{150}(17)$	L	–	$\frac{-10.3\div-18.5}{-12.0}(9)$	$\frac{-0.3\div-1.5}{-1.0}(9)$	$\frac{0.5-3}{2}$	–	–	–	–

Note. P, primary; PS, pseudosecondary; S, secondary: b, water-carbon dioxide; c, water-salt; d, single-phase liquid or gas inclusions; L, into liquid; G, into gas; G–L, critical (disappearance of gas/liquid boundary). Dash, not determined.

from the Olimpiadinskoe deposit are represented in the summary Table 1. Homogenization temperatures of primary and pseudosecondary inclusions in quartz (generations I) of preore metasomatites from nonauriferous quartz–mica–sulfide associations varies in the range of 220 to 325 °C during homogenization into a liquid phase. In some inclusions containing CO_2, depressurization of the vacuole takes place before complete homogenization, which is most likely related to the increase in internal fluid pressure. In primary and pseudosecondary inclusions, fluid with a salinity 10–16 wt.% (NaCl-equiv.) was captured, and the liquid phase composition of inclusions is determined by Na chlorides. In secondary inclusions, homogenization temperatures do not exceed 190 °C, the liquid phase is dominated by chlorides of K and Na, and the average salinity is 3 wt.% (Table 1).

In ore stage quartz II from quartz–gold–arsenopyrite–pyrite–pyrrhotite associations, homogenization temperatures of primary and pseudosecondary inclusions reach 470 °C, ranging from 260 to 470 °C. They homogenize into gas, liquid and with critical phenomena. In these inclusions, fluid with salinity of 9.5 to 20 wt.% (NaCl-equiv.) was captured and its composition is determined by chlorides of Mg and Na. In secondary inclusions, daughter salt crystals (L_{H_2O} + G + Cr) are conserved with fluid of salinity more than 30 wt.%, and the salt background of the fluid is determined by chlorides of Na and Ca. Homogenization temperature varied in the range of 160–240 °C. When homogenization proceeded into liquid, daughter crystals dissolved in this temperature range (Table 1), which appeared again when the temperature decreased. Secondary gas-liquid (L_{H_2O} + G) inclusions homogenized in the range of 150–210 °C. On homogenized into a liquid phase, the salinity of the fluid varied from 0.5 to 3 wt.%, and fluid composition was determined by the chlorides of K and Na.

Lower homogenization temperatures of primary and pseudosecondary inclusions (240–300 °C) were found in quartz of generation III from quartz–gold–antimony associations. The salinity of these fluids ranged from 5.5 to 8 wt.%, and the salinity background was determined by chlorides of Na and Mg. Secondary inclusions were homogenized into a liquid phase in the range of temperatures from 120 to 190 °C, salinity background is represented by chlorides of K and Na. Fluid pressure during mineral formation at the Olimpiadinskoe deposit varied in the range of 0.6 to 2.5 kbar (Table 1).

In quartz of IV generation from thin quartz-calcite veinlets, the lowest homogenization temperatures in the range of 110–180 °C with homogenization into liquid were observed; salinity varied from 0.5 to 3 wt.% (NaCl-equiv.) with the salinity background determined by chlorides of K and Na (Table 1).

In the fluid inclusions of quartz and sulfides from the Olimpiadinskoe deposit the content of PGE was determined (PGE—Ir, Ru, Rh, Pt, Pd), which averages 83 and 90 ppb, respectively. The proportion of platinum and palladium in the fluids of quartz and sulfides is also close and amounts to 87 and 76%, respectively. The content of rhenium (Re), which was found in the fluids of quartz and sulfides differs significantly. On the average, Re content in quartz is 47 ppb in the range of 0.4 to 442.9 ppb, and is considerably less than 8 ppb, varying from 0.1 to 65 ppb (Tomilenko et al., 2008).

Composition of gas phase of fluid inclusions in quartz and sulfides. The composition of gas component of fluids from the Olimpiadinskoe deposit was determined using Raman spectroscopy and gas chromatography–mass spectrometry (GC–MS).

The Raman spectroscopy was used to determine the gas phase of 88 individual fluid inclusions in quartz (Table 2). The presence of three main components was revealed: CO_2, CH_4 и N_2, the content of which varies in wide ranges. Nonauriferous fluids are dominated by CO_2 and CH_4, with varying ratios CO_2/CH_4 in the range from 0.1 to 20.4 (on the average 2.5, $n = 24$); in quartz gold–arsenopyrite–pyrrhotite associations, the ratio CO_2/CH_4 varies from 0.05 to 8.3 (on the average 1.4, $n = 34$) and in quartz–gold–antimony parageneses the ratio CO_2/CH_4 varies from 0.01 to 46.5 (on the average 4.4, $n = 23$).

The results of gas chromatography-mass spectrometry in fluid inclusions from 18 samples of quartz and sulfides (Table 3) showed the presence of water, carbon dioxide, a wide range of hydrocarbon compounds and their derivatives: aliphatic (alkanes, alkenes), cyclic (cycloalkanes, cycloalkenes, arenes, polycyclic aromatic hydrocarbons), oxygenated (alcohols, ethers, aldehydes, ketones, carboxylic acids, dioxanes, furans), as well as nitrogenated and sulfonated compounds. Table 3 shows the most representative results, and for Fig. 3*a*, *b*, analysis of 18 samples were used. The total number of detected compounds in the fluid of early nonauriferous associations reaches 138, 179 in quartz–gold–sulfide and 199 in quartz–gold–antimony, i.e., the quantity of revealed compounds increases from early to late fluids (Table 3).

In the same direction (from early to late parageneses) the ratio of volatile components also varies. Fluids of nonauriferous associations are dominated by CO_2 with less amounts of S- and N-bearing compounds at lower water content (Fig. 3*A*). Fluids of gold-bearing arsenopyrite–pyrrhotite parageneses are enriched with hydrocarbons, S- and N-bearing compounds and CO_2, and fluids of quartz–gold–antimony associations are dominated by H_2O and CO_2 with lower contents of hydrocarbons and S- and N-bearing compounds. It is worth noting that fluids from quartz–gold–arsenopyrite–pyrrhotite associations contain halogenated hydrocarbons, such as 1-fluorobutane (C_4H_9F), 1-chlorobutane (C_4H_9Cl), 1.1-dichlor-1-fluorobunate ($C_2H_3Cl_2F$), etc., whose content is by an order of magnitude higher than in fluids of early and late parageneses. The group of sulfonated compounds is dominated by SO_2, and nitrogenated, by N_2, the proportion of which may amount to 98 and 99%, respec-

Table 2. Microthermometric characteristics and composition of gas phase of individual fluid inclusions in quartz from the Olimpiadinskoe gold deposit (Raman spectroscopy data)

No. well/depth, m	No. inclusion	Melting T of $CO_2 \pm CH_4 \pm N_2$, °C	Homogenization T of $CO_2 \pm CH_4 \pm N_2$, °C	Type of homogenization	Content, mol.%			CO_2/CH_4
					CO_2	CH_4	N_2	
Nonauriferous quartz–mica–sulfide associations								
183/216.5	1	–63	–4.5	L	70.0	14.5	15.5	4.8
	2	–67.5	–8.5	L	65.4	14.3	20.3	4.6
	3	–59.3	–4.2	G	83.1	5.9	11.0	14.1
	4	–	–92.5	L	15.3	78.3	6.4	0.2
	5	–	–89.3	L	9.4	85.0	5.6	0.1
	6	–	–90.6	L	15.2	69.7	15.1	0.2
	7	–	–102	L	9.1	81.6	9.3	0.1
510/817	1	–66	–8.5	L	62.0	35.5	2.5	1.8
	2	–63	–9.3	L	66.3	29.6	4.1	2.2
	3	–67.3	–11	L	69.1	30.0	0.9	2.3
	4	–69.1	–10.5	L	70.8	28.7	0.5	2.5
	5	–	–123	L	9.6	72.4	18.0	0.1
	6	–	–140	L	10.6	70.8	18.7	0.2
	7	–	–135.5	L	6.7	81.3	12.0	0.1
	8	–	–120.8	L	5.9	90.5	3.6	0.1
Quartz–gold–arsenopyrite–pyrrhotite associations								
504/94.05	1	–68.5	–23.3	L	30.9	23.5	45.6	1.3
	2	–62.3	–20.3	L	48.1	15.6	36.3	3.1
	3	–71.8	–31.5	G	39.4	9.6	51.0	4.1
	4	–69.4	–22.6	G–L	23.1	6.4	70.5	3.6
	5	–	–89	L	39.0	15.7	45.3	2.5
	6	–	–113	G	21.8	12.8	65.4	1.7
	7	–	–122.5	L	10.3	40.1	49.6	0.3
1823/601.8	1	–69.8	–1.5	L	33.0	28.0	39.0	1.2
	2	–81	–3.5	L	36.0	23.7	40.3	1.5
	3	–73	–8.2	L	30.3	27.8	41.9	1.1
	4	–	–93.1	L	4.1	40.1	55.8	0.1
	5	–	–79.5	L	2.3	70.5	27.2	0.03
	6	–	–83.4	G	0	63.0	37.0	–
Quartz–gold–antimony associations								
503/202.9	1	–65.1	–0.3	L	59.3	29.8	10.9	2
	2	–68.4	–7.9	L	70.8	21.3	7.9	3.3
	3	–59.8	–3.1	G	60.4	19.5	20.1	3.1
	4	–	–111	L	10.4	85	4.6	0.1
	5	–	–121.3	G	6.5	87.4	6.1	0.1
	6	–	–94.5	L	4.8	90.3	4.9	0.05
503/473.5	1	–59.3	–11.4	L	71.0	18.2	10.8	3.9
	2	–61.8	–14.5	G	78.3	7.7	14	10.2
	3	–58.4	–9.6	L	80.3	10.5	9.2	7.6
	4	–63.4	–15.9	G	85.8	6.3	7.9	13.6
	5	–	–96.3	L	14.6	78.5	6.9	0.2
	6	–	–101.7	G	9.0	83.9	7.1	0.1

Note. L, into liquid; G, into gas; G–L, critical (disappearance of gas/liquid boundary). Dash, not determined.

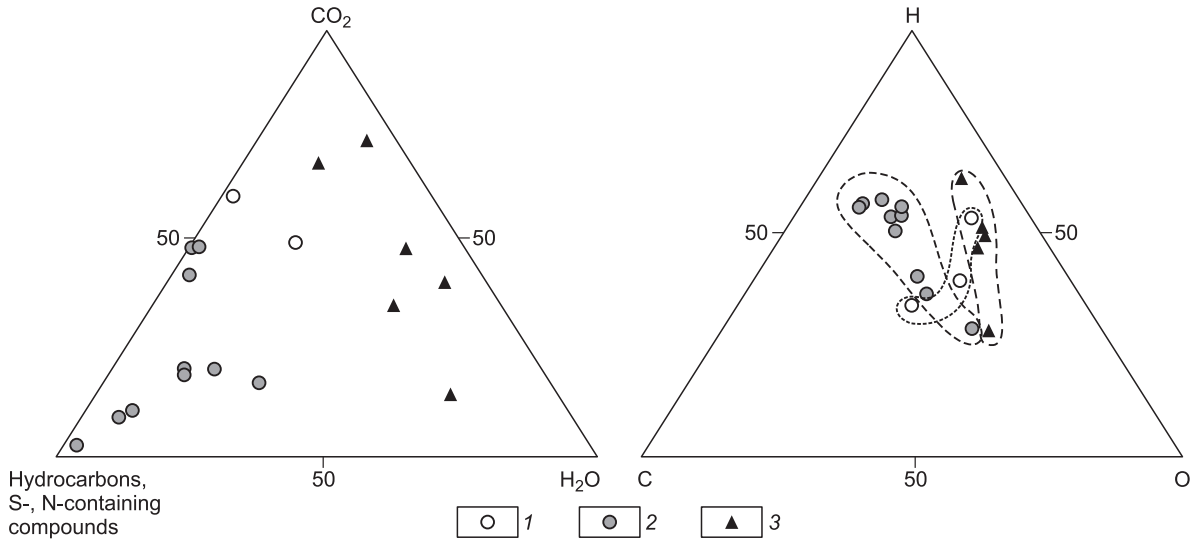

Fig. 3. Composition of gas component of fluid inclusions from the Olimpiadinskoe deposit from gas chromatography–mass spectrometry data. *1–3*, mineral associations: *1*, nonauriferous quartz–mica–sulfide; *2*, quartz–gold–arsenopyrite–pyrrhotite; *3*, quartz–gold–antimony.

tively. All fluids of the group of carboxylic acids contains acetic acid, the fraction of which ranges from 5.0 to 36.5% in nonauriferous associations, 10.4 to 75.5% in quartz-gold-arsenopyrite associations, and 3.6 to 27.7% in quartz–gold–antimony associations.

Isotopic composition of sulfide sulfur. Results of isotopic analysis of sulfide sulfur from quartz veins (55 samples) are summarized in Table 4 and shown in Fig. 4. The isotopic composition of sulfur ranges from 2.7 to 13.0‰. The isotopic composition of sulfur in arsenopyrite varies in the same wide range from 1.5 to 12.9‰. Narrower ranges of $\delta^{34}S$ values were found in pyrite and antimonite from 5.8 to 8.8 and from 4.5 to 10.4‰, respectively. The value of $\delta^{34}S$ of sphalerite falls in the same range 8.8‰. It is worth noting that isotope-light values of $\delta^{34}S$ were determined in the root part of the gold-richest orebody No. 4 from the Olimpiadinskoe deposit. Arsenopyrite from the depth of 817 m (well 510-817, Table 4) showed the values of $\delta^{34}S$ = 1.5‰, from the depth of 514 m, 2.4‰ (well 1823-514, Table 4), and the value of $\delta^{34}S$ = 2.7‰ was determined in pyrrhotite from the depth of 618 m (well 182-618a, Table 4). The greatest number (~87%) of $\delta^{34}S$ values fall in the ranges of 5.4 to 11.0‰, varying no more than 6‰.

Isotopes of helium. In the fluid inclusions of quartz III from quartz–gold–antimony mineral association (sample 503-202.9) with the content of Au = 10.8 ppm and Sb = 4.42%, the content of helium isotopes (^4He and ^3He) was found to be 56×10^{-6} and 2.8×10^{-12} cm^3/g, respectively, and the $^3He/^4He$ ratio was 0.05×10^{-6}.

The age of the deposit formation. To determine the age of formation of the Olimpiadinskoe deposit, we selected potassium-bearing minerals (sericite and muscovite) from nonauriferous quartz–mica–sulfide, quartz–gold–arsenopyrite–pyrrhotite and quartz–gold–antimony associations. $^{40}Ar/^{39}Ar$ studies were carried out on 16 samples taken from 9 wells in the range of depths from 39 to 718.5 m of orebody No. 4. The Ar–Ar age of formation of nonauriferous associations ranges 808.4 ± 7.7–817.1 ± 6.3 Ma, quartz–gold–arsenopyrite–pyrrhotite parageneses, 758.0 ± 6.0–803.0 ± 6.1 Ma, and quartz–gold-antimony associations, 660.0 ± 19.0–795.2 ± 5.8 Ma (Table 5, Fig. 5).

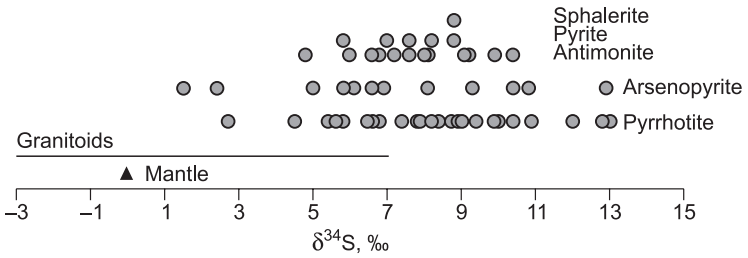

Fig. 4. Sulfur isotopic composition of sulfides from the Olimpiadinskoe gold-ore deposit. Sulfur isotopic composition of granitoids is borrowed from (Ohmoto and Rye, 1979).

Table 3. Composition (in rel.%) and number (in parentheses) of volatiles extracted at single mechanical shock destruction fluid inclusions in minerals from the Olimpiadinskoe gold deposit (gas chromatography–mass spectrometry data)

Name of components	Mineral associations							
	Nonauriferous quartz-mica sulfide		Quartz–gold–arsenopyrite–pyrrhotite			Quartz–gold–antimony		
	Quartz I	Quartz I	Quartz II	Arsenopyrite I	Arsenopyrite II	Quartz III	Antimonite	Calcite
	183-216.5	1823-548	504-94.05	504-293.8	503-39	OC-3-1	OC-3-1	OC-3-1
Aliphatic hydrocarbons								
Paraffins (alkanes)	5.11 (22)	3.98 (20)	8.53 (21)	12.93 (20)	7.52 (17)	3.77 (19)	11.96 (19)	3.60 (17)
Olefins (alkenes	0.92 (14)	3.75 (13)	0.79 (12)	4.81 (19)	5.62 (21)	0.55 (23)	0.39 (22)	0.33 (22)
Cyclic hydrocarbons								
Cycloalkanes, cycloalkenes, arenes, PAH	0.78 (17)	4.47 (13)	0.68 (14)	2.68 (21)	4.26 (19)	0.17 (24)	0.83 (28)	0.29 (27)
Oxygenated hydrocarbons								
Ethers, esters, alcohols	0.43 (9)	3.57 (9)	0.83 (12)	2.0 (12)	5.80 (11)	0.39 (19)	0.68 (19)	0.44 (17)
Aldehydes	1.31 (17)	7.88 (21)	1.37 (20)	9.62 (21)	17.93 (21)	0.94 (21)	0.92 (22)	0.77 (22)
Ketones	0.81 (13)	3.14 (14)	0.53 (15)	4.58 (15)	6.31 (14)	0.40 (20)	0.34 (14)	0.31 (21)
Carboxylic acids	1.84 (9)	0.54 (5)	0.80 (7)	18.87 (14)	15.71 (14)	1.76 (14)	1.00 (14)	0.09 (14)
Heterocyclic compounds								
Dioxanes, furans	0.16 (7)	0.20 (11)	0.04 (8)	0.42 (14)	0.87 (13)	0.03 (15)	0.15 (15)	0.04 (14)
Nitrogenated compounds								
Nitrogen, ammonia, nitriles	18.35 (10)	6.39 (15)	36.18 (12)	7.89 (18)	14.03 (18)	3.01 (21)	2.35 (18)	14.28 (19)
Sulfonated compounds								
H_2S, SO_2, CS_2, COS, thiophenes	0.70 (10)	2.67 (15)	0.63 (12)	2.63 (23)	5.52 (18)	0.20 (20)	1.76 (23)	0.17 (24)
Halogenated hydrocarbons: Cl, F, Br	0.18	0.56	0.03	2.12	0.09	0.02	0.05	0.02
Inorganic compounds								
CO_2	50.45	61.22	49.23	19.80	9.35	48.81	14.43	35.38
H_2O	19.05	2.17	0.36	13.71	7.04	39.97	65.17	44.28
The number of identified components	130	138	135	179	168	198	196	199
Ratios								
Alkanes/alkenes	5.2	1.1	10.8	2.7	1.3	6.9	30.9	11.0
$CO_2/CO_2 + H_2O$	0.7	0.9	0.9	0.6	0.6	0.6	0.2	0.4

DISCUSSION AND RESULTS

Generalization of data obtained in the study of fluid inclusions in the minerals from the unique Olimpiadinskoe deposit in the Yenisei Ridge allows a conclusion that two types fluids—water-carbon dioxide and carbon dioxide hydrocarbon—simultaneously or sequentially, participated in its formation. The terms "fluid" after F.A. Letnikov (2001, 2006) means essentially gas, water-gas and water phase in association with petrogenic and ore elements.

Hydrothermal activity at the Olimpiadinskoe deposit started from the formation of pre-ore metasomatites consisting of nonauriferous or weakly auriferous quartz-mica-sulfide associations. The temperature of formation of these parageneses ranged from 220 to 325 °C and fluid pressure varied from 0.6 to 2.2 kbar, the salinity of fluid in pseudosecondary inclusions also varied from 10 to 16 wt.%, NaCl-equiv. (Table 1). Gas chromatography mass spectrometry data (Table 3) show that water and carbon dioxide are constantly present in the fluid, i.e., this fluid can be attributed to water-carbon dioxide type. The quartz grains of pre-ore metasomatites from the deposit underwent repeated deformations after their formation, which were accompanied by the entrapment of new groups of inclusions during healing of cracks. This was marked by the appearance of two generations of secondary inclusions: gas and gas-liquid with

Table 4. Sulfur isotopic composition of sulfides from the Olimpiadinskoe gold deposit

Sample	Mineral	$\delta^{34}S$, ‰ (CDT)	Sample	Mineral	$\delta^{34}S$, ‰ (CDT)
503-4.5	Pyrrhotite	8.7	503-38.6	Arsenopyrite	10.4
503-38.6	Pyrrhotite	9.4	503-39	Arsenopyrite	5.8
503-41	Pyrrhotite	10.4	503-453	Arsenopyrite	6.6
503-49	Pyrrhotite	6.8	503-458.3	Arsenopyrite	5.0
503-153.8	Pyrrhotite	5.4	503-473.5	Arsenopyrite	8.1
503-209.7	Pyrrhotite	13.0	504-6.5	Arsenopyrite	5.8
503-226.0	Pyrrhotite	8.9	506-334.7	Arsenopyrite	6.9
503-260.5	Pyrrhotite	10.0	510-817	Arsenopyrite	1.5
503-303	Pyrrhotite	12.8	511-322	Arsenopyrite	12.9
503-415.5	Pyrrhotite	12.0	511-591.4	Arsenopyrite	10.8
504-94.05	Pyrrhotite	10.9	186-365	Arsenopyrite	9.3
505-58	Pyrrhotite	9.9	1823-514	Arsenopyrite	2.4
506-145	Pyrrhotite	7.8	1823-528.4	Arsenopyrite	6.1
506-161.4	Pyrrhotite	8.4	503-4.5	Antimonite	7.2
506-323.5	Pyrrhotite	7.9	503-41	Antimonite	9.2
507-20	Pyrrhotite	8.2	503-64.6	Antimonite	8.1
182-618a	Pyrrhotite	2.7	503-206	Antimonite	8.0
186-365	Pyrrhotite	9.0	503-209.7	Antimonite	9.1
186-562	Pyrrhotite	4.5	503-260.5	Antimonite	9.9
1823-514	Pyrrhotite	7.4	503-473.5	Antimonite	10.4
1823-528.4	Pyrrhotite	5.8	503-488.2	Antimonite	6.8
OPR-2-8	Pyrrhotite	5.6	506-145	Antimonite	6.0
OPR-2-7	Pyrrhotite	6.6	182-618a	Antimonite	6.6
OPR-2-3	Pyrrhotite	6.5	1823-601.8	Antimonite	7.6
183-216.5	Pyrite	7.0	OC-3-2	Antimonite	4.8
503-49	Pyrite	7.6	OC-3-1	Antimonite	9.1
503-153.8	Pyrite	5.8	510-718.5	Sphalerite	8.8
505-58	Pyrite	8.8			
506-161.4	Pyrite	8.2			

Note. Sulfur isotopic composition of sulfides was determined in the Analytical Center, V.S. Sobolev Institute of Geology and Mineralogy SB RAS, Novosibirsk. Analysts V.N. Reutsky, M.N. Kolbasova.

their T–P–X-characteristics (Tables 1, 3). According to Ar–Ar dating, pre-ore metasomatites were formed during the period of 808.4 ± 7.7–817.1 ± 6.3 Ma (Table 5).

Quartz–gold–arsenopyrite–pyrrhotite association of the ore stage of hydrothermal activity at the deposit formed at higher temperatures which already reached 470 °C when homogenization into liquid and gas took place, and with critical phenomena, i.e., heterophase fluid was trapped by inclusions. Pressure change in the range of 1.1–2.5 kbar (Table 1) resulted in boiling of the polycomponent water-carbon-dioxide-hydrocarbon fluid and its separation into essentially water fraction (inclusions of $L_{H_2O} + G$, $L_{H_2O} \pm L_{CO_2 \pm CH_4 \pm N_2} + G$ types) and gas and liquid-gas (inclusion of $G_{H2O} \pm G_{CH_4 \pm N_2 \pm CO_2}$, $L_{CH_4 \pm N_2 \pm CO_2} + G$ types). During the process of boiling, mainly CH_4 и N_2 pass into a gas phase, because their coefficients of solubility in water are by 1–2 orders lower than those of CO_2 (Naden and Shephard, 1989; Kryazhev, 2010). Boiling of fluid is an effective reason for crystallization of ore minerals, including gold (Ermakov and Dolgov, 1979; Roedder, 1987; Mishra and Pal, 2008). Fluid salinity in primary and pseudosecondary inclusions varies in the range of 9.5 to 20 wt.%, NaCl-equiv. Quartz veins with gold–arsenopyrite–pyrrhotite mineralization were repeatedly influenced by later essentially gas (or gas-liquid) high-saline or low-saline fluids, which is indicated by the generation of secondary inclusions (Table 1, S-b, S-c, S-d). Raman spectroscopy data show that gas inclusions contain CO_2, CH_4 and N_2 in different ratios (Table 3). The secondary high salinity (H_2O + NaCl + $CaCl_2$) inclusions with daughter crystals ($L_{H_2O} + G + Cr$, Fig. 2*c*) were found in gold-bearing quartz from the root part of orebody No. 4 at the Olimpiadinskoe deposit at the depths lower than 500 m (well 182, depth 618 m, well 1823, depth 514, 523.8 and 601.8 m). The presence of concentrated (>30 wt.%) NaCl–$CaCl_2$-bearing

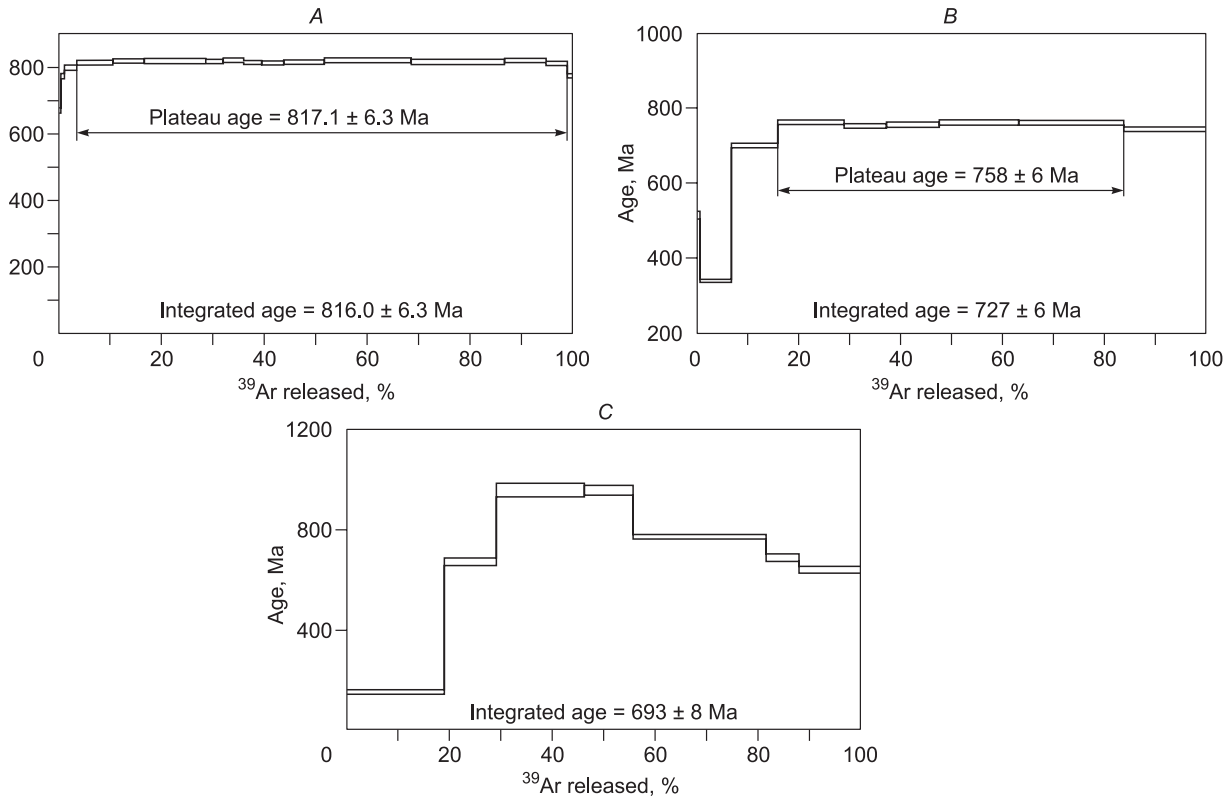

Fig. 5. Spectra of $^{40}Ar/^{39}Ar$ ages of mineral associations from the Olimpiadinskoe deposit. *A*, nonauriferous quartz–sulfide–mica association, well 1823/548; *B*, quartz–gold–arsenopyrite–pyrite–pyrrhotite association, well 1823/601.8; *C*, quartz–gold–antimony association, well 503/473.5.

fluids at gold ore deposits of the world is a characteristic feature of Proterozoic hydrothermal systems, which associate with granitoid plutons (Xu, 2000; Shelton et al., 2004; Bhattacharya and Panigrahi, 2011). We think that post-magmatic hydrothermal solutions of nearby granitoids, which surround the ore field of the deposit in a semicircle, could be the source of highly saline fluid. Similar highly saline type of fluid was found at the Panimba gold ore deposit, which is also in the zone of influence of the Chirimba granitoid complex (Gibsher et al., 2017).

The formation of the early quartz–gold–arsenopyrite–pyrrhotite association of the ore stage proceeded in the time range from 803.0 ± 6.1 to 758.0 ± 6.0 Ma, where the ages from 795 to 784 Ma predominate (Table 5, Fig. 5). The early main gold-bearing quartz–arsenopyrite–pyrrhotite association is replaced by later quartz–gold–antimony association which was formed during the period from 795.2 ± 5.8 to 660.0 ± 19.0 Ma with the predominance of young ages in the range of 757–718 Ma. The age of recrystallized arsenopyrite aggregates in association with antimony mineralization by the Re/Os method is 689 ± 28 Ma (Borisenko et al., 2014). The comparison of $^{40}Ar/^{39}Ar$ ages of studied parageneses of pre-ore and ore stages shows that hydrothermal activity at the Olimpiadinskoe deposit continued in the time range of at least 150 Ma (from 817 to 660 Ma) (Gibsher et al., 2019). The age of crystallization of the multiphase Chirimba granitoid pluton exposed in the south and southwest of the ore field (Fig. 1) from some authors' data, is 840 ± 150 Ma (Volobuev et al., 1973), and according to others, is 870 ± 35 Ma (Novozhilov et al., 2014), 868.9 ± 6.5 Ma (Sazonov et al., 2016), 761.5 ± 8.0 Ma (Vernikovskaya et al., 2002). Cooling of this pluton to closure temperature of the $^{40}Ar/^{39}Ar$ biotite system occurred at 721.4 ± 1.6 Ma (Vernikovskaya et al., 2002). These data suggest that the period from the introduction and crystallization to cooling and rising to the upper levels of the Earth's crust of the Chirimba pluton in the time range from 868 to 721 Ma lasted at least 150 Ma. Such a large pluton like Chirimba, could provide slower cooling of the ore deposition region and thus maintain a longer functioning of rising ore-bearing solutions. The data obtained by Novozhilov et al. (2014) also indicate a long period of formation of the Olimpiadinskoe deposit, which is nearly 179 Ma. Our Ar–Ar dating of the formation of the Olimpiadinskoe deposit is close to the age of development of tectonomagmatic processes associated with the epochs of formation and evolution riftogenic structures and manifestations of intraplate magmatism at the turn of three epochs (Nozhkin et al., 2011).

Despite the different TPX-parameters of mineral parageneses of different ages from the Olimpiadinskoe deposit, they have one common feature they were exposed to different degrees of influence of carbon dioxide-hydrocarbon flu-

Table 5. Isotope $^{40}Ar/^{39}Ar$ dating of mineralization at the Olimpiadinskoe deposit (Yenisei Ridge)

Well/depth, m	Mineral	Plateau age, Ma	Content in the interval		
			Au, ppm	As, %	Sb, %
Nonauriferous quartz–mica–sulfide association					
183/216.5	Muscovite	810.1 ± 6.5	Negligible		
1823/548	Muscovite	817.1 ± 6.3	Negligible		
35/111	Muscovite	808.4 ± 7.7	Negligible		
Quartz–gold–arsenopyrite–pyrrhotite association					
503/303	Muscovite	784.5 ± 6.2	4.0	0.02	0.0
504/94.05	Sericite	792.4 ± 6.3	6.40	0.07	0.01
506/323.5	Sericite	790.0 ± 6.0	1.6	0.84	0.01
507/20	Sericite	792.4 ± 6.0	0.6	0.0	0.0
510/718.5	Sericite	795.8 ± 6.2	4.0	0.26	0.0
186/365	Sericite	803.0 ± 6.1	16.2	1.86	0.01
1823/514.8	Sericite	788.0 ± 6.1	1.5	0.4	0.0
1823/601.8	Sericite	758.0 ± 6.0	4.1	0.43	0.0
Quartz–gold–antimony association					
503/39	Sericite	727.0 ± 6.0	21.6	2.16	1.78
503/49	Sericite	718.8 ± 5.6	0.3	0.06	0.01
503/202.9	Sericite	757.7 ± 5.9	10.8	0.02	4.42
503/260.5	Sericite	795.2 ± 5.8	0.5	0.02	0.17
503/473.5	Sericite	660.0 ± 19.0	1.2	11.5	0.26

Note. Ar–Ar determinations were performed in the Analytical Center of V.S. Sobolev Institute of Geology and Mineralogy SB RAS (Novosibirsk). Analysts A.V. Travin, A.V. Ponomarchuk.

ids. The reducing character of these fluids is confirmed by the presence of such components as paraffin (alkanes) and olefins (alkenes) (Table 3). Some authors (Norman et al., 2002; Blamey, 2012) propose to use the alkane/alkene ratios for reconstructing the redox potential of fluids. When alkanes dominate, the fluid is reduced, and when alkenes are predominant, the fluid is oxidized. According to gas chromatography-mass spectrometry data (Table 3), the alkane-alkene ratios in the fluids from the Olimpiadinskoe deposit range from 1.1 to 30.9, i.e., the fluids correspond to a reduced state. The reduced character of the fluids is also indicated by the water content (from 0.4 to 13.7 rel.%, Table 3), especially in the quartz–gold–arsenopyrite associations of the ore stage, whereas in the later antimony-bearing association, the water content increased from 40 to 65 rel.% (Table 3), showing that the reduced fluids were replaced by oxidized. The data of A.A. Yaroshevskii (2006) suggest that a low water content in the fluid is a prerequisite for the occurrence of reducing environment in the mineral-forming medium.

Carbon dioxide in various amounts is constantly present in the fluids from the Olimpiadinskoe deposit, as shown by both the data of the Raman spectroscopy (Table 2) and gas chromatography-mass spectrometry (Table 3). At the depths of the Earth's crust, all the component of the fluid, including CO_2, are in a supercritical state (Savage et al., 1995; Gorbatyi and Bondarenko, 2007; Letnikov et al., 2018). A supercritical fluid is something average between a liquid and gaseous state and demonstrates a unique reaction ability to transport and deposit ore substance (Letnikov et al., 2018). Carbon dioxide, as a supercritical fluid, is used for the analysis of nonvolatile substances which cannot be analyzed by the gas chromatography method. For this purpose, supercritical gas chromatography is used (Taylor and Miller, 2010). These authors report that CO_2 in a mixture methanol, ethanol, and 1- and 2-butanol has a high dissolving ability. SO_2 may also have the same properties. With an increase in H_2O in the fluid, the dissolving ability of CO_2 and SO_2 drops (Taylor and Miller, 2010). In such a scenario under natural conditions, sulfides and gold are to be precipitated.

In the fluids from the Olimpiadinskoe deposit the content of PGE (Ir, Ru, Rh, Pt, Pd) and Re were determined, which indicate two types of fluid (Gibsher et al., 2018). We think that fluids with elevated contents of platinoids (~90 ppb) were supplied through the zones of tectonic faults from the deeper horizons of the continental crust. Fluids with a contrasting rhenium content in the regions of mineral formation are related to carbonaceous sedimentary rocks (Baioumy et al., 2011). Ore-bearing rocks from the Olimpiadinskoe deposit contain carbonaceous shale (Li, 2003). Rhenium, which was detected in the fluids from the deposit with contents ranging from 0.1 to 423 ppb, could be borrowed from host rocks during the fluid—carbonaceous shale interaction.

Reduced fluids can accumulate and transport significant masses of native elements, including gold (Gizé and Macdonald, 1993; Emsbo and Koenig, 2007). On the basis of conducted experiments, it was shown that gold and ore elements are transported by hydrocarbons that act as ore fluid (Zezin et al., 2007, 2011; Zakirov et al., 2008; Williams-Jones et al., 2009; Fuchs et al., 2015; Migdisov et al., 2017). The gas chromatography-mass spectrometry data showed that fluid inclusions in the native gold from the Sovetskoye deposit at the Yenisei Ridge contain significant amounts (>80 rel.%) of CO_2, hydrocarbons, S-, N-bearing compounds and considerably less water (<13 rel.%) (Bul'bak et al., 2018a,b).

Experimental data in the system Fe–C–S at high T–P-parameters showed that t fluid phase has a complex composition and is characterized by the presence of not only inorganic components (CO_2, H_2O, N_2, SO_2, CS_2, COS) but also organic compounds, such as heavy hydrocarbons and oxygen-bearing analogs (Zhimulev et al., 2015). The complex composition of fluids from the Olimpiadinskoe deposit is also indicated by the quantity of detected compounds which increases from 138 in pre-ore metasomatites, to 179 in quartz–gold–sulfide and 199 in antimony-bearing associations. This increase is, most likely, related to the supply of additional portions of chemical compounds in the fluid from other sources.

In endogenic processes, volatile components retain high mobility (Archibalt et al., 2001; Williams-Jones and Heinrich, 2005; Malyshev, 2008). The idea that gases can play their part in transporting metals was first reported on the basis of theoretical researches (Krauskopf, 1957). Then, finding of gold in appreciable amounts in gas inclusions from gold ore deposits of Argentina and Indonesia led the authors (Ulrich et al., 1999) to the conclusion that gases play an important part in the transport of metals, including gold. The highly mobile gaseous carbon dioxide-hydrocarbon fluids discovered in the minerals from the Olimpiadinskoe deposit were the reason for the occurrence of scattered gold ore mineralization in the large volume of quartz-carbonate-mica shales with layers of limestones, which play the roles of geochemical barriers. The carbonate-bearing rocks of the deposit were influenced by ore-forming fluids containing up to 19 rel.% carboxylic acids (Table 3). According to (Greenwood et al., 2013), carboxylic acids are, on the one hand, highly soluble in water and are the transport medium. On the other hand, these acids at the same time increase the porosity of host rocks, which also contributes to the migration of organoelement compounds (OEC) in reduced fluids. The fluids transporting metals into ore-deposition zones should contain such elements as Cl, F, B, P, S, N (Williams-Jones et al., 2009). This set of elements was detected in the fluids from the Olimpiadinskoe deposit by the gas chromatography–mass spectrometry analysis (Table 3).

Sulfide sulfur of arsenopyrite and pyrrhotite, which are the main gold concentrators at the Olimpiadinskoe deposit, is enriched with heavy isotope $\delta^{34}S$ in the range of 1.5 to 13‰. Antimonite, pyrite and sphalerite showed narrower ranges of $\delta^{34}S$, 4.8 to 10.4 ‰ (Table 4, Fig. 4). Our data on $\delta^{34}S$ sulfides of quartz veins from the deposit are comparable with the earlier estimations at the Olimpiadinskoe deposit (Konstantinov and Kosovetz, 2007; Serdyuk et al., 2010; Kryazhev, 2017). The obtained isotopic data show that sulfur in the ores from the deposit (from 1.5 to 13.0‰) can be obtained by "averaging" sulfur from host rocks and these values suggest their crustal origin (Ohmoto and Rye, 1979).

In the fluid inclusions of quartz from the quartz–gold–antimony association from the Olimpiadinskoe deposit we determined the content of helium isotopes, $^3He = 2.8 \times 10^{-12}$ and $^4He = 56 \times 10^{-6}$ cm^3/g, at these parameters the ratio $^3He/^4He = 0.05 \times 10^{-6}$. It was shown in (Ikorsky et al., 2006, 2014; Vetrin et al., 2003) that mantle fluid is rich in ^3He, and the crustal, in ^4He. Therefore, the ratio $^3He/^4He$ can be used to diagnose the source of this element. The fraction of mantle helium (^3He), calculated by the procedure from (Khalenev, 2010; Prasolov et al., 2018), in the fluids of antimony-bearing association of the Olimpiadinskoe deposit equals 0.25%. This supports our assumption that auriferous fluids are crustal fluids.

CONCLUSIONS

The Olimpiadinskoe gold deposit was formed by metal-bearing oxidized water-carbon dioxide and reduced carbon dioxide-hydrocarbon fluids in the range of temperatures from 220 to 470 °C and pressures from 0.6 to 2.5 kbar.

The deposit was formed in the time interval from 817 to 660 Ma and fits the time interval of crystallization and cooling of the multiphase Chirimba granitoid pluton. The hydrothermal activity of fluids at the deposit continued for no less than 100 Ma.

Fluids of auriferous mineral associations contained CO_2, hydrocarbons, S-, N-, halogenated compounds that are potentially capable of transporting ore elements, including Au, platinum group elements and are a positive indicator of gold content.

The Olimpiadinskoe deposit with the unique reserves of gold at the Yenisei Ridge was formed owing to the combination of a number of favorable factors, including the geological position and long-term activity of reduced fluids supplied from the depths of the Earth's crust.

We are thankful to the anonymous reviewers for their constructive suggestions and comments taken into account in the final version of the manuscript.

The work was performed under the State assignment, project 0330-2016-0005, and with support from the Russian Science Foundation project 14-17-00602П.

REFERENCES

Afanas'eva, Z.B., Ivanova, G.F., Miklishanskii, A.Z., Romashova, T.V., Kolesov, G.M., 1995. Geochemical characteristics of the tungsten

mineralization of the Olimpiadinskoe gold-sulfide deposit (Yenisei Ridge). Geokhimiya, No. 1, 29–47.

Archibald, S.M., Migdisov, A.A., Williams-Jones, A.E., 2001. The stability of Au-chloride complexes in water vapor at elevated temperatures and pressure. Geochim. Cosmochim. Acta 65 (23), 4413–4423.

Baioumy, H.M., Eglinton, L.B., Peucker-Ehrenbrink, B., 2011. Rhenium-osmium isotope and platinum group element systematics of marine vs. non-marine organic-rich sediments and coals from Egypt. Chem. Geol. 285 (1–4), 70–81.

Bakker, R.J., 2001. FLUIDS: new software package to handle microthermometric data and to calculate isochores, in: Noronha, F., Doria, A., Guedes A. (Eds.), Abstracts. Faculdade de Ciencias do Porto, Departamiento de Geologia, Memoria, Vol. 7, pp. 23–25.

Baranova, N.N., Afanas'eva, Z.B., Ivanova, G.F., Mironova, O.F., Kolpakova, N.N., 1997. Mineralization at the Olympiada Au–(Sb–W) deposit: evidence from mineral parageneses and fluid inclusions. Geochem. Int. 35 (3), 239–249.

Bhattacharya, S., Panigrahi, M.K., 2011. Heterogeneity in fluid characteristics in the Ramagiri–Penakacherla sector of the Eastern Dharwar Craton: implications to gold metallogeny. Russian Geology and Geophysics (Geologiya i Geofizika) 52 (11), 1436–1447 (1821–1834).

Blamey, N.J.F., 2012. Composition and evolution of crustal, geothermal and hydrothermal fluids interpreted using quantitative fluid inclusion gas analysis. J. Geochem. Exp. 116–117, 17–27.

Borisenko, A.S., 1977. Studying the salt composition of solutions of gas-liquid inclusions in minerals by the method of cryometry. Geologiya i Geofizika, No. 8, 16–27.

Borisenko, A.S., Sazonov, A.M., Nevolko, P.A., Naumov, E.A., Tessalina, S., Kovalev, K.R., Sukhorukov, V.P., 2014. Gold deposits of the Yenisei Ridge (Russia) and age of its formation. Acta Geol. Sin.-Engl. 88 (Suppl. 2), 686–687.

Brown, P.E., Lamb, W.M., 1989. P–V–T properties of fluids in the system $H_2O \pm CO_2 \pm NaCl$: new graphical presentations and implications for fluid inclusion studies. Geochim. Cosmochim. Acta 53, 1209–1231.

Bul'bak, T.A., Tomilenko, A.A., Sazonov, A.M., Gibsher, N.A. Ryabukha, M.A. Khomenko, M.O., 2018a. Hydrocarbons in the fluid inclusions of native gold, in: Asian Current Research on Fluid Inclusions VIII (ACROFI-VIII), pp. 19–20.

Bul'bak, T.A., Tomilenko, A.A., Sazonov, A.M., Gibsher, N.A., Ryabukha, M.A., Khomenko M.O., 2018b. Hydrocarbons of fluid inclusions in the minerals of ores of gold deposits of the Yenisei Ridge, in: Abstracts of the XVIII All-Russian Conference on Thermobarogeochemistry (100th of Yu.A. Dolgov) [in Russian]. Mineral. Museum RAS, Moscow, pp. 32–34.

Buryak, V.N., 1982. Metamorphism and Ore Formation [in Russian]. Nedra, Moscow.

Duan, Z., Moller, N., Weare, J.H., 1996. A general equation of state for supercritical fluid mixtures and molecular dynamics simulation of mixture PVTX properties. Geochim. Cosmochim. Acta 60 (7), 1209–1216.

Dubessy, J., Poty, B., Ramboz, C., 1989. Advances in C–O–H–N–S fluid geochemistry based on micro-Raman spectrometric analysis of fluid inclusions. Eur. J. Miner. 1, 517–534.

Emsbo, P., Koenig, A.E., 2007. Transport of Au in petroleum: evidence from the northern Carlin trend, Nevada, in: Andrew, C.J., Borg, G. (Eds.), Digging Deeper, Proceedings of the Ninth Biennial SGA Meeting. Irish Association for Economic Geology, Dublin, pp. 695–698.

Ermakov, N.P., Dolgov, Yu.A., 1979. Termobarogeochemistry [in Russian]. Nedra, Moscow.

Fuchs, S., Schumann, D., Williams-Jones, A.E., Vali, H., 2015. The growth and concentration of uranium and titanium minerals in hydrocarbons of the Carbon Leader Reef, Witwatersrand Supergroup, South Africa. Chem. Geol. 393–394, 55–66.

Genkin, A.D., Lopatin, V.A., Savel'ev, R.A., Safonov, Yu.G., Sergeev, N.B., Kerin, A.L., Tsepin, A.I., Amshtuts, H., Afanas'eva, Z.B., Vagner, F., Ivanova, G.F., 1994. Gold ores of the Olimpiadinskoe deposit (Yenisei Ridge, Siberia). Geologiya Rudnykh Mestorozhdenii 36 (2), 111–136.

Genkin, A.D., Wagner, F.E., Krylova, T.L., Tsepin, A.I., 2002. Gold-bearing arsenopyrite and its formation conditions at the Olympiada and Veduga gold deposits (Yenisei Range, Siberia). Geol. Ore Deposit 44 (1), 52–68.

Gibsher, N.A., Tomilenko, A.A., Sazonov, A.M., Ryabukha, M.A., Timkina, A.L., 2011. The Gerfed gold deposit: fluids and PT-conditions for quartz vein formation (Yenisei Ridge, Russia). Russian Geology and Geophysics (Geologiya i Geofizika) 52 (11), 1461–1473 (1851–1867).

Gibsher, N.A., Ryabukha, M.A., Tomilenko, A.A., Sazonov, A.M., Khomenko, M.O., Bul'bak, T.A., Nekrasova, N.A., 2017. Metal-bearing fluids and the age of the Panimba gold deposit (Yenisei Ridge, Russia). Russian Geology and Geophysics (Geologiya i Geofizika) 58 (11), 1366–1383 (1721–1741).

Gibsher, N.A., Kozmenko, O.A., Tomilenko, A.A., Sazonov, A.M., Ryabukha, M.A., 2018. Elements of the platinum group and rhenium in the fluids of the Olimpiadinskoe gold deposit (Yenisei Ridge, Russia), in: Abstracts of the XVIII All-Russian Conference on Thermobarogeochemistry (the 100th anniversary of Yu.A. Dolgov) [in Russian]. Mineral. Museum RAS, Moscow. pp. 37–38.

Gibsher, N.A., Sazonov, A.M., Travin, A.V., Tomilenko, A.A., Ponomarchuk, A.V., Sil'yanov, S.A., Nekrasova, N.A., Shaparenko, E.O., Ryabukha, M.A., Khomenko, M.O., 2019. Age and duration of the formation of the Olimpiada gold deposit (Yenisei Ridge, Russia). Geochem. Int. 5, 593–599.

Gizé, A.F., Macdonald, R., 1993. Generation of compositionally atypical hydrocarbons in CO_2-rich geologic environment. Geology 21 (2), 129–132.

Gorbatyi, Yu.E., Bondarenko, G.V., 2007. Supercritical state of water. Sverkhkriticheskie Flyuidy: Teoriya i Praktika 2 (2), 5–19.

Greenwood, P.F., Brocks, J.J., Grice, K., Schwark, L., Dick, J.M., Evans, K.A., 2013. Organic geochemistry and mineralogy. I. Characterisation of organic matter associated with metal deposits. Ore Geol. Rev. 50, 1–27.

Groves, D.I., Goldfarb, R.J., Santosh, M., 2016. The conjunction of factors that lead to formation of giant gold provinces in non-arc setting. Geosci. Front. 7 (3), 303–314.

Ikorsky, S.V., Gannibal, M.A., Avedisyan, A.A., 2006. High-temperature impregnation of helium into fluid inclusions in minerals: experiments with quartz and nepheline. Dokl. Earth Sci. 411 (1), 1299–1302.

Ikorsky, S.V., Kamensky, I.L., Avedisyan, A.A., 2014. Helium isotopes in contact zones of alkaline intrusions of different size: A case study of the alkaline-ultrabasic Ozernaya Varaka intrusive and the Lovozero massif of nepheline syenites (Kola Peninsula). Dokl. Earth Sci. 459 (2), 1543–1547.

Khalenev, V.O., 2010. The Isotopic Composition of Helium and Argon, as a Criterion for the Ore-Bearing Intrusions of the Norilsk Region. PhD Thesis [in Russian]. St. Petersburg.

Kirgintsev, A.N., Trushnikova, L.I., Lavrent'eva, V.G., 1972. Solubility of Inorganic Substances in Water. Handbook [in Russian]. Khimiya, Leningrad.

Konstantinov, M.M., Kosovets, T.N., 2007. Isotopic-geochemical features of sulfide sulfur of gold deposits in terrigenous strata. Rudy i Metally 5, 49–57.

Koz'menko, O.A., Palesskii, S.V., Nikolaeva, I.V., Tomas, V.G., Anoshin, G.N., 2011. Improvement of the method of chemical preparation of geological samples in Carius tubes for the determination of elements of the platinum group and rhenium. Analiticheskii Kontrol' 15 (4), 378.

Krauskopf, K.B., 1957. The heavy metal content of magmatic vapor at 600 °C. Econ. Geol. 52 (7), 786–807.

Kryazhev, S.G., 2010. Current problems of the theory and practice of thermobarogeochemistry. Rudy i Metally 2, 38–46.

Kryazhev, S.G., 2017. Genetic Models and Criteria for Prediction of Gold Deposits in Carbon-Terrigenous Complexes. SciD [in Russian]. TsNIGRI, Moscow.

Kryazhev, S.G., Grinenko, V.A., 2007. The isotopic composition and sources of sulfur in gold-sulphide deposits of the Yenisei Ridge, in: Abstracts of the XVIII Symposium on Geochemistry of Isotopes [in Russian]. GEOKhI RAN, Moscow, p. 37.

Letnikov, F.A., 2001. Ultradeep fluid systems of the Earth and problems of ore formation. Geol. Ore Deposit 43 (4), 259–273.

Letnikov, F.A., 2006. Fluids in endogenic processes and problems of metallogeny. Russian Geology and Geophysics (Geologiya i Geofizika) 47 (12), 1271–1281 (1296–1307).

Letnikov, F.A., Shumilova, T.G., Medvedev, V.Ya., Ivanova, L.A., 2018. Transport and crystallization of noble platinum in supercritical C–O–H fluid. Dokl. Earth Sci. 479 (2), 460–462.

Li, L.V., 2003. Olympiada Deposit of Disseminated Gold-Sulfide Ores [in Russian]. KNIIGiMS, Krasnoyarsk.

Li, L.V., Kruglov, G.P., Shokhina, O.I., Verbitsky, B.P., 1984. The role of lithological and structural factors in the localization of vein-impregnated mineralization in the over-intrusive zone. Geologiya Rudnykh Mestorozhdenii, No. 1, 83–88.

Malyshev, A.I., 2008. Gas diffusion in the evolution of magmatic systems. Dokl. Earth Sci. 422 (1), 1113–1115.

Migdisov, A.A., Guo, X., Xu, H., Williams-Jones, A.E., Sun, C.J., Vasyukova, O., Sugiyama, I., Fuchs, S., Pearce, K., Roback, R., 2017. Hydrocarbons as ore fluids. Geochem. Perspect. Lett. 5, 47–52.

Mishra, B., Pal, N., 2008. Metamorphism, fluid flux and fluid evolution relative to gold mineralization in the Hutti-Mashi Greenstone Belt, Eastern Dharwar Craton, India. Econ. Geol. 103, 801–827.

Naden, J., Shepherd, T.J., 1989. Role of methane and carbon dioxide in gold deposition. Nature 343, 793–795.

Norman, D.I., Blamey, N., Moore, J.N., 2002. Interpreting geothermal processes and fluid sources from fluid inclusion organic compounds and CO_2/N_2 ratios, in: Proceeding of 27th Workshop on Geothermal Reservoir Engineering, pp. 234–241.

Novozhilov, Yu.I., Gavrilov, A.M., 1999. Gold-Sulfide Deposits in Carbon-Terrigenous Strata. Olimpiadinskoe Deposit [in Russian]. TSNIGRI, Moscow.

Novozhilov, Yu.I., Gavrilov, A.M., Yablokova, S.V., Aref'eva, V.A., 2014. High-volume gold deposits in black shale strata—geological, structural, genetic, geochemical features, ore processing technologies. Rudy i Metally 3, 51–64.

Nozhkin, A.D., Borisenko, A.S., Nevol'ko, P.A., 2011. Stages of Late Proterozoic magmatism and periods of Au mineralization in the Yenisei Ridge. Russian Geology and Geophysics (Geologiya i Geofizika) 52 (1), 124–143 (158–181).

Ohmoto, H., Rye, R.O., 1979. Isotopes of sulfur and carbon, in: Geochemistry of Hydrothermal Ore Deposit. Wiley, New York, pp. 509–567.

Pal'yanova, G.A., Sobolev, E.S., Reutsky, V.N., Bortnikov, N.S., 2016. Upper Triassic pyritized bivalve mollusks from the Sentachan orogenic gold–antimony deposit, eastern Yakutia: Mineralogy and sulfur isotopic composition. Geol. Ore Deposit 58 (6), 456–464.

Petrov, V.G., 1974. Gold Conditions in the Northern Part of the Yenisei Ridge (Trans. IGG SO AN SSSR, Issue 69) [in Russian]. Nauka, Novosibirsk.

Prasolov, E.M., Sergeev, S.A., Belyatsky, B.V., Bogomolov, E.S., Gruzdov, K.A., Kapitonov, I.N., Krymsky, R.Sh., Khalenev, V.O., 2018. Isotopic systematics of He, Ar, S, Cu, Ni, Re, Os, Pb, U, Sm, Nd, Rb, Sr, Lu, and Hf in the rocks and ores of the Norilsk deposits. Geochem. Int. 56 (1), 46–64.

Prokof'ev, V.Yu., Afanas'eva, Z.B., Ivanova, G.F., Buaron, M.K., Marinyak, H., 1994. Study of fluid inclusions in the minerals of the Olympiada Au–(Sb–W) deposit, Yenisei Ridge. Geokhimiya 4, 1012–1029.

Roedder, E., 1987. Fluid Inclusions in Minerals, Vol. 1 [in Russian]. Mir, Moscow.

Ryabukha, M.A., Gibsher, N.A., Tomilenko, A.A., Bul'bak, T.A., Khomenko, M.O., Sazonov A.M., 2015. P-T-X parameters of metamorphogene and hydrothermal fluids, isotopy and age of the Bogunai gold deposit, southern Yenisei Ridge (Russia). Russian Geology and Geophysics (Geologiya i Geofizika) 56 (6), 903–918 (1153–1172).

Savage, P.E., Gopalan, S., Mizan, T.I., Martino, C.J., Brock, E.E., 1995. Reactions at supercritical conditions: applications and fundamentals. AIChE J. 41 (7), 1723–1778.

Sazonov, A.M., Kremenetskii, A.A., 1994. Geochemistry of gold in the metamorphic complex of the Northern Ladoga area. Geokhimiya 10, 1451–1464.

Sazonov, A.M., Ananyev, A.A., Poleva, T.V., Khokhlov, A.N., Vlasov, V.S., Zvyagina, E.A., Fedorova, A.V., Tishin, P.A., Leontyev, S.I., 2010. Gold-ore metallogeny of the Yenisei Ridge: geological-structural province, structural types of ore fields. Zhurnal SFU. Tekhnika i Tekhnologiya 3 (4), 371–395.

Sazonov, A.M., Nekrasova, N.A., Zvyagina, E.A., Tishin, P.A., 2016. Geochronology of granites, surrounding schists and ores of the Panimba gold deposit (the Yenisei Ridge). Zhurnal SFU. Tekhnika i Tekhnologiya 9 (2), 174–188.

Serdiuk, S.S., Komorovsky, Yu.E., Zverev, A.I., Oyaber, V.K., Vlasov, V.S., Babushkin, V.E., Kirilenko, V.A., Zemlyansky, S.A., 2010. Gold Deposits Models of Yenisean Siberia [in Russian]. SFU, Krasnoyarsk.

Shelton, K.I., McMenamg, T.A., van Hees, E.H., Falck, H., 2004. Deciphering the complex fluid history of a greenstone-hosted gold deposit: fluid inclusion and stable isotope studies of the Giant Mine, Yellowknife Northwest Territories, Canada. Econ. Geol. 99 (8), 1643–1663.

Sokol, A.G., Palyanov, Y.N., Tomilenko, A.A., Bul'bak, T.A., Palyanova, G.A., 2017. Carbon and nitrogen speciation in nitrogen-rich C–O–H–N fluids at 5.5–7.8 GPa. Earth Planet. Sci. Lett. 460, 234–243.

Taylor, L., Miller, L., 2011. Supercritical fluid chromatography with packed columns. Sverkhkriticheskie Fluidy. Teoriya i Praktika 6 (1), 69–83.

Thiéry, R., van den Kerkhof, A.M., Dubessy, J., 1994. υX properties of CH_4–CO_2 and CO_2–N_2 fluid inclusions: modeling for T < 31 °C and P < 400 bars. Eur. J. Miner. 6 (6), 753–771.

Tolstikhin, I.N., Prasolov, E.M., 1971. The method of studying the isotopes of noble gases from microinclusions in rocks and minerals, in: Studies of Mineral-Forming Solutions and Melts on Inclusions in Minerals (Trans. VNIISIMS, Issue 14) [in Russian]. VNIISIMS, Aleksandrov, pp. 86–98.

Tomilenko, A.A., Gibsher, N.A., 2001. Peculiarities of fluid composition in the mineralized and barren zones of the Sovetskoe quartz–gold deposit, Yenisei Mountain Range based on fluid inclusion study. Geochem. Int. 39 (2), 142–152.

Tomilenko, A.A., Gibsher, N.A., Koz'menko, O.A., Palesskii, S.V., Nikolaeva, I.V., 2008. Lanthanides in fluid inclusions, quartz, and greenschists from auriferous and barren quartz-vein zones of the Sovetskoe quartz-gold deposit, Yenisei Range, Russia. Geochem. Int. 46 (4), 402–408.

Tomilenko, A.A., Gibsher, N.A., Dublyansky, Y.V., Dallai, L., 2010. Geochemical and isotopic properties of fluids from gold-bearing and barren quartz veins of the Sovetskoye gold deposit (Siberia, Russia). Econ. Geol. 105 (2), 375–394.

Tomilenko, A.A., Chepurov, A.I., Sonin, V.M., Bul'bak, T.A., Zhimulev, E.I., Chepurov, A.A., Timina, T.Yu. Pokhilenko, N.P., 2015. The synthesis of methane and heavier hydrocarbons in the system graphite-iron-serpentine at 2 and 4 GPa and 1200 °C. High Temp. High Press. 44 (6), 451–465.

Travin, A.V., 2016. Thermochronology of Early Paleozoic collisional and subduction–collisional structures of Central Asia. Russian Geology and Geophysics (Geologiya i Geofizika) 57 (3), 434–450 (553–574).

Ulrich, T., Günther, D., Heinrich, C.A., 1999. Gold concentrations of magmatic brines and the metal budget of porphyry copper deposits. Nature 399, 676–679.

Vetrin, V.R., Kamenskii, I.L., Ikorskii, S.V., Gannibal, M.A., 2003. Juvenile helium in Archean enderbites and alkaline granites of the Kola Peninsula. Geochem. Int. 41 (7), 631–636.

Vernikovskaya, A.E., Vernikovsky, V.A., Sal'nikova, E.B., Datsenko, V.M., Kotov, A.B., Kovach, V.P., Travin, A.V., Yakovleva, S.Z., 2002. Yeruda and Chirimba granitoids (Yenisei Ridge) as indicators of Neoproterozoic collisions. Geologiya i Geofizika (Russian Geology and Geophysics) 43 (3), 259–272 (245–259).

Volobuev, M.I., Stupnikova, N.I., Zykov, S.I., 1973. Yenisei Ridge, in: Polovinkina, Yu.I. (Ed.), Geochronology of the USSR [in Russian]. Nedra, Leningrad, Vol. 1, pp. 189–201.

Williams-Jones, A.E., Heinrich, C.A., 2005. 100th Anniversary Special Paper: Vapor transport of metals and the formation of magmatic-hydrothermal ore deposits. Econ. Geol. 100 (7), 1287–1312.

Williams-Jones, A.E., Bowell, R.J., Migdisov, A.A., 2009. Gold in solution. Elements 5 (5), 281–287.

Xu, G., 2000. Fluid inclusions with NaCl–$CaCl_2$–H_2O composition from the Cloncurry hydrothermal system, NW Queensland, Australia. Lithos 53 (1), 21–35.

Yaroshevskii, A.A., 2006. Possible geochemical conditions of local reducing environments in the Earth's crust and upper mantle. Geochem. Int. 44 (3), 308–309.

Zakirov, I.V., Dadze, T.P., Sretenskaya, N.G., Kashirtseva, G.A., 2008. Experimental data on gold solubility in low-density hydrothermal fluids. Dokl. Earth Sci. 423 (2), 1492–1494.

Zezin, D.Yu., Migdisov, A.A., Williams-Jones, A.E., 2007. The solubility of gold in hydrogen sulfide gas: an experimental study. Geochim. Cosmochim. Acta 71 (12), 3070–3081.

Zezin, D.Yu., Migdisov, A.A., Williams-Jones, A.E., 2011. The solubility of gold in H_2O–H_2S vapour at elevated temperature and pressure. Geochim. Cosmochim. Acta 75 (18), 5140–5153.

Zhimulev, E.I., Sonin, V.M., Bul'bak, T.A., Chepurov, A.I., Tomilenko, A.A., Pokhilenko, N.P., 2015. Volatile compounds of sulfur in the Fe–C–S system at 5.3 GPa and 1300 °C. Dokl. Earth Sci. 462 (1), 527–532.

Editorial responsibility: A.V. Travin